ORIGINAL ARTICLE

Mussel-mimicking sulfobetaine-based copolymer with metal tunable gelation, self-healing and antibacterial capability

Miroslav Mrlík [a],*, **Mário Špírek** [b], **Jassim Al-Khori** [c], **Ali Abdulrahman Ahmad** [c], **Jaroslav Mosnaček** [d], **Mariam AlAli AlMaadeed** [e], **Peter Kasák** [f],*

[a] *Centre of Polymer Systems, University Institute, Tomas Bata University in Zlin, Trida T. Bati 5678, 760 01 Zlin, Czech Republic*
[b] *Department of Biology, Faculty of Medicine, Masaryk University, 62500 Brno, Czech Republic*
[c] *Maersk Oil Research and Technical Center, Doha, Qatar*
[d] *Polymer Institute, Slovak Academy of Sciences, Dubravska cesta 9, 84541 Bratislava, Slovakia*
[e] *Materials Science and Technology Program, Qatar University, P.O. BOX 2713, Doha, Qatar*
[f] *Center for Advanced Materials, Qatar University, P.O. BOX 2713, Doha, Qatar*

Abstract In the present study, the sulfobetaine-based copolymer bearing a dopamine functionality showed gel formation adjusted by the application of metal salts for gelation and various values of pH. Normally, the liquid-like solution of the sulfobetaine-based copolymer and metal cross-linkers is transformed to a gel-like state upon increasing the pH values in the presence of Fe^{3+} and Ti^{3+}. Metal-induced coordination is reversible by means of the application of EDTA as a chelating agent. In the case of Ag^+ ions, the gel is formed through a redox process accompanied with the oxidative coupling of the dopamine moieties and Ag^0 particle formation. Mussel-mimicking and metal-dependent viscoelastic properties were observed for Fe^{3+}, Ti^{3+}, and Ag^+ cross-linking agents, with additionally enhanced self-healing behavior in comparison with the covalently cross-linked IO_4^- analogues. Antibacterial properties can be achieved both in solution and on the surface using the proper concentration of Ag^+ ions used for gelation; thus, a tunable amount of the Ag^0 particles are formed in the hydrogel. The cytotoxicity was elucidated by the both MTT assay on the NIH/3T3 fibroblast cell line and direct contact method using human dermal fibroblast cell (F121) and shows the non-toxic character of the synthesized copolymer.

© 2017 The Authors. Production and hosting by Elsevier B.V. on behalf of King Saud University. This is an open access article under the CC BY-NC-ND license (http://creativecommons.org/licenses/by-nc-nd/4.0/).

* Corresponding authors.
E-mail addresses: mrlik@cps.utb.cz (M. Mrlík), peter.kasak@qu.edu.qa (P. Kasák).

1. Introduction

The investigation of many biological materials enabling controllable reinforcement of their adhesive, mechanical, or friction properties upon interaction with metal ions (Gil and Hudson, 2004; Mart et al., 2006; Phadke et al., 2012) captures a great deal of attention. One of the most investigated systems is mussel byssus thread, in which highly concentrated catecholic units from 3,4-dihydroxyphenylalanine (DOPA) in the mussel foot protein 1 (mfp-1) form coordination complexes with Fe^{3+} ions with particle-like structures (Freitas and Stadler, 1987; Holten-Andersen et al., 2009). These structures reinforce the materials and are involved in its hardness and high elasticity. The concept of utilizing the strong coordination capability and possible oxidation of the catecholic fragment by different metals was utilized in the formation of adhesive materials to different surfaces (Li et al., 2015), to water treatment (Yu et al., 2015) or in metal cross-linked hydrogels (Lee et al., 2006; Zeng et al., 2010) while various polymers such as polyethylene glycol (PEG) Holten-Andersen et al., 2011; Pop-Georgiewski et al., 2011, chitosan (Yavvari and Srivastava, 2015) and other polymeric systems (Sedó et al., 2013) were used.

One of key parameters dictating the resulting properties of the catecholic based materials is the coordination with metals into complexes or the oxidation ability of the dopamine units with an applied metal. It was assumed that in mfp-1 Fe^{3+} forms hexadentate mononuclear coordination complexes with DOPA moieties and, moreover, different metals, such as Ti, B, Zn, and Mn were utilized in the complexation studies as well (Xu, 2013). Generally, the stiffness of the hydrogels cross-linked by the metal ions mentioned above mainly in the case of Fe^{3+} was comparable to that obtained for covalently cross-linked hydrogels (Holten-Andersen et al., 2011). The dynamic behavior of coordination complexation of the systems of the DOPA derivative and metals contributes to their self-healing properties in biological systems (Holten-Andersen et al., 2007; South and Lyon, 2010) as well as in synthetic hydrogel systems (Sedó et al., 2013; Harrington et al., 2010).

The concept of supramolecular metal-based self-healing materials depends on employing non-covalent coordination bonds to generate networks, which are able to be reversibly healed (Freitas and Stadler, 1987; Stadler and Freitas, 1986). Additionally, supramolecular interactions can affect the material properties of polymer-based hydrogels (viscosity, moduli) as well as the internal ordering of the polymer chain (Brunsveld et al., 2001; de Greef and Meijer, 2008; Hoeben et al., 2005; Bassett et al., 2016). The enhanced dynamic behavior of these systems contributes to their application as self-healing materials in bioengineering and biomedical purposes. Currently, the self-healing hydrogels, able to be spontaneously recovered after they are damaged, started to be developed because the self-healing phenomenon together with tunable mechanical properties enables them to be applied as versatile smart systems (Phadke et al., 2012; Roy et al., 2010; Guvendiren et al., 2012; Fletcher et al., 2011; Piest et al., 2011).

Sulfobetaine polymer-based materials possess highly ionic characters with balanced charges between the sulfate and quaternary ammonium group in each monomer unit and strong electrostatic interactions with water (Sobolčiak et al., 2011). Mainly due to these features, they are used for protein stabilization (Yan et al., 2006), drug delivery (Jin et al., 2014), non-fouling surfaces (Zhang et al., 2006, 2009a; Stach et al., 2011), hydrogel materials (Zhang et al., 2009b; Kasák et al., 2011) and further progressive applications (Ilcikova et al., 2015; Pei et al., 2012; Mrlík et al., 2016).

So far, sulfobetaine polymers with catecholic DOPA units were only used for immobilization on surfaces, such as hydrophobic polylactic acid (Yang et al., 2016), polypropylene (PP), polydimethylsiloxane (PDMS), polystyrene (PS), nylon, polyvinyl chloride (PVC), and poly(methyl methacrylate) (PMMA), gold, hydrophilic silica (Sundaram et al., 2014), stainless steel (Sin et al., 2014) or glass (Lia et al., 2008). In the above mentioned cases, the DOPA derivates are used as a joining agent for attachment to various substrates through catecholic OH groups and no study on sulfobetaine based hydrogel structure formation based on metal ions has been done so far.

In this study, the developed polymeric material combining both zwitterionic and catecholic structures facilitates non-fouling and non-toxic properties as well as a tunable cross-linking ability. The sulfobetaine-based copolymer SBE-DAM was synthesized by free radical copolymerization of [2-(methacryloyloxy)ethyl]dimethyl-(3-sulfo propyl)ammonium betaine (SBE) and dopamine methacrylamide (DAM). Further, the gelation process SBE-DAM with different metal ions (Ti^{3+}, Fe^{3+}, Ag^+) was investigated. After the addition of Ti^{3+} and Fe^{3+} ions, UV–vis measurements and oscillatory shear measurements determined that the network structure development accompanied with increasing pH values. In the case of the Ag^+ ion, oxidative coupling of catechol unit was accompanied by the formation of Ag particles. Self-healing properties were elucidated by oscillatory shear measurements and showed fast and complete recovery in the case of the Ti^{3+} based hydrogel. Different states of water influencing the viscoelastic properties and self-healing ability were also investigated. Antibacterial properties of the hydrogel can be achieved and adjusted by the amount of embedded Ag particles. Furthermore, SBE-DAM showed non-toxic character, as proved by the MTT assay on the NIH/3T3 fibroblast cell line, making it particularly interesting for further biomedical and (bio)engineering applications.

2. Experimental

2.1. Materials

$FeCl_3$, $TiCl_3$, $AgNO_3$, Nitric acid 36% (Sigma-Aldrich, USA), $Na_2B_4O_7 \cdot 10\ H_2O$ (98%, Aldrich), $NaHCO_3$ (Aldrich), dopamine HCl (98%, Aldrich), [2-(methacryloyloxy)ethyl] dimethyl-(3-sulfopropyl)ammonium betaine, (SBE, Aldrich 97%), methacrylic anhydride (99%, Aldrich), 2,2′-azobis(2-methyl propionamide) dihydrochloride (AIBA, Aldrich 97%), and ethyl acetate (Spectrolab, p.a.) were used as received.

2.2. Synthesis of dopamine methacrylamide monomer (DAM)

Synthesis of the monomer was carried out according to a slightly modified procedure from the literature (Lee, 2008) as follows.

A two necked flask was filled with 5 g of $Na_2B_4O_7 \cdot 10\ H_2O$, 2 g of $NaHCO_3$ and 2.5 g of dopamine HCl (13.2 mmol) and filled with argon. 50 mL of degassed H_2O was added via a septum to dissolve these components. 2.3 mL of methacrylic anhydride (14.5 mmol) in 20 mL of THF was added dropwise for 1 h. The reaction was stirred for 16 h under argon at ambient temperature. Then, the reaction mixture was washed twice with 20 mL of ethyl acetate and the organic layers were discarded. The aqueous layer was acidified with 6 N HCl to a pH of 1–2, and the crude product was extracted twice with 20 mL of ethyl acetate. Collected organic layers were dried over Na_2SO_4, the solvent was evaporated to half volume and white crystals were formed. Recrystallization in hexane and ethyl acetate was carried out and the monomer was obtained with a 40% yield.

^{1}H NMR (d_6-DMSO): δ 8.78 (1H, Ar—O*H*), 8.67 (1H, Ar—O*H*), 7.6 (1H, CON*H*), 6.62–6.34 (3H, Ar—*H*), 5.67 (1H, =C—*H*), 5.35 (1H, =C—*H*), 3.23 (2H, C*H2*NH), 2.55 (2H, Ar—C*H2*), 1.86 (3H, C=C(C*H3*)). These results are in agreement with the literature (Ham et al., 2011).

2.3. Synthesis of sulfobetaine-based copolymer (SBE-DAM)

A 50 mL Schlenk flask was filled with 109 mg of DAM (0.5 mmol), 1.25 g of SBE (4.5 mmol), 14 mg of AIBA (0.06 mmol) and filled with argon together with a stir bar. 10 mL of 0.5 M aq. NaCl was added and flask was closed with a stopper. Three freeze-pump-thaw cycles were applied and the flask was filled with argon. The reaction mixture was stirred for 6 h at 60 °C. After cooling, the mixture was dialyzed trice against 0.2 M NaCl and with ultrapure water for 2 days using a permeable cellulose membrane (MWCO 1000 Da Spectra/Por® Spectrum Laboratories, Inc., CA, USA). The solution with sparingly soluble residue was lyophilized and an off-white solid was obtained in 71% yield. GPC: (M_w = 48,000, PDI = 2.4). Methacrylic-based monomers ensure random copolymerization and a molar ratio in the resulting copolymer SBE-DAM between monomers SBE and DAM was calculated from the ^1H NMR spectrum and it was estimated as 92.5/8.5.

2.4. Characterization

^1H NMR was recorded on a Varian Gemini 300 instrument at 298 K with a working frequency of 300 MHz. Chemical shifts are reported in ppm downfield, and the solvent was used as a reference. Coupling patterns were designated as s-singlet, d-doublet, t-triplet, and m-multiplet. Coupling constants are given in Hz. The concentration of samples was approximately 10 mg in 0.7 mL of solvent.

To evaluate molecular weight and polymer chain distributions, the HPLC Breeze system (Waters) was employed, operated in GPC mode, and coupled with a refractive index detector (RI) (Waters 2414) at 40 °C. Separation was conducted using a Shodex Ohpak SB-806 M HQ bed column (300 × 8 mm, 13 μm particles) at 40 °C. The mobile phase was water with a flow rate of 1.0 mL/min and the injection volume was 100 μL. The GPC system was calibrated with narrow pullulan standards ranging from 180 to 708,000 g mol^{-1}. All data processing was carried out using Empower software. Polymer samples of approximately 3 mg were dissolved in 1 mL of deionized water and filtered prior to analysis.

Fourier transform infrared spectroscopy (FTIR) (Nicolet 6700, USA) in the attenuated total reflectance (ATR) mode within the wave number range of 4000–500 cm^{-1} using a germanium crystal was utilized for structural investigation when copolymer was mixed with KBr and measurements were performed on the pellets using 64 scans.

2.5. Preparation of metal ions cross-linked gels and covalently cross-linked gels

The copolymer SBE-DAM was prepared according to the procedure described in the previous section and was used for all further experiments.

The Fe^{3+}-cross-linked gel was made as follows: SBE-DAM solution with a copolymer concentration 200 mg mL^{-1}, which corresponds to 20 mM of catecholic groups in 3.5 wt.% aqueous NaCl, was mixed to obtain a volume of copolymer solution of 1 mL. Then, FeCl$_3$ was added, to establish the molar ratio between the catecholic groups to Fe at 1:3, and the green color of the mixture was developed. This mixture has a pH of 5, and predominantly mono-catecholato-Fe^{3+} complexes were

obtained. Further, after the addition of a small amount of 0.1 M NaOH in saline solution, the pH increased to 8 and the immediate process of gelation connected to the color change was observed. In this case, the bis-catecholato-Fe^{3+} complexes were formed. However, when the pH was set to 12 by titration with 0.1 M NaOH in saline solution, a solid gel consisting mostly of tris-catecholato-Fe^{3+} complexes was obtained. The pH of the samples was measured using a WTW 330i pH meter (Germany).

The preparation of Ti^{3+}-cross-linked gels was the same as in the previous case. However, only the addition of the 0.1 M NaOH promotes the gelation effect of the mixture connected to the rapid change of viscosity of the sample. Further, the titration of the mixture results in the better elastic properties of catecholato-Ti^{3+}-cross-linked gels.

The last cross-linked gel was prepared using various amounts of AgNO$_3$ (50, 100 and 200 mg) in the Tris buffer medium (100 mM, pH 8.5) to prevent AgCl precipitation. The copolymer solution was used in a concentration of 200 mg mL^{-1} and the molar ratio between the catecholic groups and Ag^+ was 1:1, 2:1 and 4:1. The gel with a molar ratio 1:1 was formed within the 45 min and contained the lowest amount of Ag^0 particles (Table 2).

For comparison of the viscoelastic properties of metal cross-linked gels, the covalently cross-linked gel was prepared as follows: the concentration of the synthesized polymer was 200 mg mL^{-1}, and NaIO$_4$ was used as a cross-linking agent. The ratio between the catecholic groups and IO$_4^-$ was 1:2. The fully covalently cross-linked gel was obtained after 5 h.

2.6. UV–vis spectrophotometry

To monitor the structural development after the addition of various metal ligand cross-linkers in solutions with different pH values, the absorbance measurements on the UV–vis spectrometer SPECORD 210 (Analytik Jena AG, Germany) to observe spectral changes for Fe^{3+} and Ti^{3+} polymer solutions with concentration 1 mg mL^{-1} were performed in the range from 300 to 1000 nm in a quartz 10 mm cuvette. The spectral changes were recorded after the continuous addition of 0.1 M NaOH solution.

2.7. Differential scanning calorimetry

The differential scanning calorimetry (DSC) measurements were performed using differential scanning calorimeter (Mettler-Toledo, Switzerland). The nitrogen gas flow rate was set to 40 mL min^{-1}. Similar hydrogels used for rheological measurement were first cut, weighed accurately and sealed in aluminum pans. The weight ranged from 4 to 5 mg. DSC curves were reached by heating from −45 to 20 °C and back with a heating rate of 3 °C min^{-1}. All experiments were performed three times, and average values were used for further investigation.

2.8. Equilibrium water content measurements

Hydrogel samples were lyophilized for one day and stored in desiccator over CaCl$_2$ at ambient temperature before weighing. Then, the equilibrium water content (EWC) was obtained for all prepared hydrogels according to Eq. (1):

$$EWC = \frac{(W_\infty - W_d)}{W_\infty} \cdot 100\% \tag{1}$$

where W_∞ is the weight of the hydrogel at equilibrium and W_d is the weight of the lyophilized hydrogel.

2.9. Viscoelastic measurements

The mechanical properties of the prepared gels were measured using a rotational rheometer MCR-502 (Anton Paar, Austria) with a parallel plate geometry of 25 mm in diameter and 500 μm at 20 °C controlled with a Peltier measuring setup. Frequency dependence of the storage (G') and elastic (G'') moduli from 0.1 to 3 Hz was measured in the linear viscoelastic region, which was established at 1% strain (γ) value.

The recovery test was performed on the samples at pH 12 prepared according to a previous procedure with the same setup at strain deformations from 0.01 to 500% at a frequency of 1 Hz followed by measurements of the time dependence of the G' at linear conditions (1% strain deformation and 1 Hz) to monitor the recovery of the storage modulus (G'). This measurement was performed at 20 °C with a total measuring time of less than 20 min to avoid dehydration of the samples (Freitas and Stadler, 1987).

2.10. Antibacterial assessment

Escherichia coli (*E. coli*) M15 bacteria cells were first cultured in 2xTY media overnight at 37 °C. The cells were diluted in fresh 2xTY media and incubated at 37 °C to reach an optical density (OD) of 1.0 at 600 nm. 1 mL of bacterial cells was collected by centrifugation at 8000g for 2 min, resuspended in 1 mL of sterile water, and centrifuged again, the washing step was repeated. Finally, the cells were diluted in sterile water to an OD of 0.007 and then 0.06 mL of the solution was mixed with 6 mg of polymer hydrogel. The suspension was incubated at room temperature for 20 min. A 0.04 mL aliquot was taken carefully, diluted by a factor of 10, and spread on solid 2xTY culture plates which were incubated overnight at 37 °C. In the case of the negative control (nontreated cells) where no cytotoxicity was expected, a dilution by a factor of 100 was used. Live cells were counted in the form of the colony forming units (cfu) and the percentage of live cells was calculated as percentage of cfu (hydrogel)/cfu(control) ∗ 100. The whole experiment was performed in triplicate.

2.11. Antimicrobial assessment using the zone of inhibition

E. coli M15 and *S. Aureus* bacteria cells were first cultured in 2xTY media overnight at 37 °C. The cells were diluted to fresh 2xTY media and incubated at 37 °C to reach an OD of 1.0 at 600 nm. Additionally, 1 mL of the bacterial cells was collected by centrifugation at 8000g for 2 min, and washed twice with sterile water, and finally the cells were diluted with sterile water ($\sim 10^7$ cells/ml). Then, 0.1 mL of the cell suspension was spread on solid 2xTY culture plates. A slice of hydrogel (5 mg) was carefully placed on the plate with the cells and incubated overnight at 37 °C. The next day, the diameter of the zone of inhibition was measured in 5 directions, and an average value was calculated. Each test was performed in triplicate.

2.12. Cytotoxicity evaluation

For extract cytotoxicity determination, the protocol according to international standard EN ISO 10993-5 using NIH/3T3 mouse embryonic fibroblast cell line (ATCC, CRL-1658), typically used cell line for cytotoxicity materials testing was performed, while human dermal fibroblast cell (F121) was used for direct method. The cultured cells were provided with Dulbecco's Modified Eagle Medium placed in tissue culture plastic flasks and incubated having CO_2 (5%) and at 37 ° C in wet atmosphere and cultivated for 24 h in contact with synthesized copolymer SBE-DAM. Dulbecco's Modified Eagle Medium – high glucose, with 10% calf serum and Penicillin/Streptomycin, 100 μg mL^{-1} (PAA Laboratories GmbH, Austria) – was used as a culture medium.

Extract preparation: Prior to extraction, the samples were disinfected at 120 °C for 40 min (Binder ED 53, Germany). SBE-DAM was extracted according to ISO 10993-12 in the amount of 0.2 g of the SBE-DAM per 1 mL of culture medium and incubated and stirred at 37 ± 1 °C for 24 h. The parent extracts (termed as 100%) were diluted in the culture medium to obtain extracts with concentrations of 100, 75, 50, 25, 10 and 5 vol.%. The extracts were used for cytotoxicity testing within 48 h.

The cells were seeded on microtitration plates (TPP, Switzerland) at a concentration of 1×10^5 cells per mL and pre-cultivated for 24 h. The culture medium was subsequently replaced with SBE-DAM extracts at a certain concentration. The cells were cultivated for 24 h in the presence of this solution. The cell viability was evaluated by a MTT assay (Invitrogen Corporation, USA). The absorbance was measured at 570 nm with an Infinite M200 Pro NanoQuant absorbance reader (Tecan, Switzerland). All of the tests were performed in quadruplicate. Cell viability was expressed as the percentage of cells present in the corresponding extract relative to cells cultivated in pure growth medium (reference, 100% viability). Values > 0.8 were assigned to no cytotoxicity, 0.6–0.8 to mild cytotoxicity, 0.4–0.6 to moderate cytotoxicity, and < 0.4 to severe cytotoxicity. The morphology of the cells was observed by an inverted Olympus phase contrast microscope (Olympus IX81, Japan).

3. Results and discussion

3.1. Synthesis

The synthesis of copolymer SBE-DAM was performed by free radical polymerization with AIBA as an initiator in 0.5 M NaCl according to Scheme 1. The product was characterized by FTIR, ^{1}H NMR and GPC analysis.

In the FTIR spectra presented in Fig. S1, Supporting information, an absorbance band belonging to the phenolic O—H stretching vibration can be observed at 3454 cm^{-1}. Signals at 3300 cm^{-1} and 1642 cm^{-1} correspond to N—H and C═O stretching vibrations of the amide group, respectively. The absorbance at 1726 cm^{-1} denotes the esteric C═O stretching vibration. Absorption bands at 1174 cm^{-1} and 1037 cm^{-1} are related to organic sulfate and the quaternary ammonium group, respectively. Absorption bands at 1481 cm^{-1} and 3010 cm^{-1} are characteristic for C—H bending and stretching vibrations of the methylene group, respectively. The ^{1}H
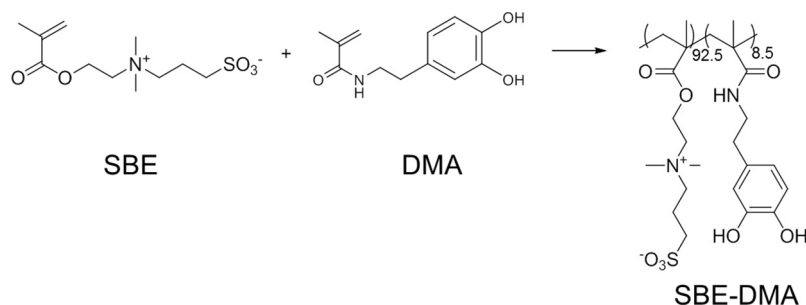
Scheme 1   Synthesis of a copolymer SBE-DAM involving: AIBA, 0.5 M NaCl, at 60 °C for 6 h.

NMR spectrum also confirmed incorporation of DAM by the presence of a chemical shift at approximately 7 ppm belonging to the aromatic proton of DAM. The peaks are assigned in Fig. S2, Supporting information. The molecular weight and dispersity of SBE-DAM determined by size exclusion chromatography were 48 kDa and 2.4, respectively. The GPC elugram shows monomodal distribution as depicted in elugram in Fig. S3, Supporting information. Relatively high polydispersity could be influenced by the tendency of the catecholamine-based polymers to oxidize or form cross-links during GPC analysis (Lee et al., 2006).

3.2. Formation of the metal induced cross-linked gel

The step-by-step coordination development of the Fe^{3+} cross-linked polymer gel network can be seen in Fig. 1. The synthesized polymer was dissolved in the NaCl solution, and, after addition of an appropriate amount of $FeCl_3$, the pH of the system was approximately 5. The absorbance spectra of this solution slightly increased without any visible peak. Such behavior represents the mono-catecholate Fe^{3+} gel formation. After the addition of a small amount of NaOH, the cross-linking reaction occurred at pH 8, resulting in the bis-catecholate Fe^{3+} gel represented by the absorption peak with a maximum at 575 nm. After further addition of NaOH, the pH of the solution increased to 12. This increase was accompanied with the formation of the tris-catecholate Fe^{3+} cross-linked gel with a visible absorption peak with a maximum at 478 nm.
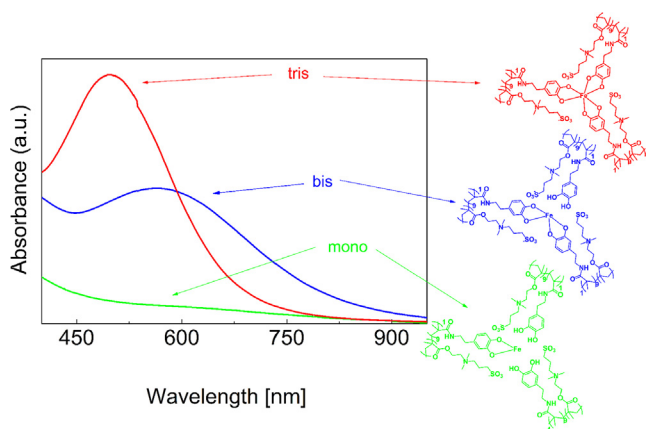
On the other hand, the formation of the Ti^{3+} cross-linked polymer gel network was considerably different (Fig. 2). When the $TiCl_3$ was added to the polymer solution, the measured pH was similar to the previous case, and the predominantly mono-catecholate Ti^{3+} gel was formed. However, continuous titration with NaOH did not result in the bis-catecholate Ti^{3+} gel, but tris-catecholate Ti^{3+} gel complexes were directly formed. However, at the same time, free catecholate-groups were still present in the system, resulting in the moderate gel stiffness. Only after reaching pH 12 by the titration, the complexation of the all catecholate-groups with the metal ion was reached. This was also confirmed by the shift of the absorption peak maximum from 480 nm at pH 8 to 462 nm at pH 12.

Unlike for the previous ions, in the case of the Ag^+ ions, the formation of covalently cross-linked gels was observed. The generation of the covalently cross-linked gels was slower than the formation of the cross-linked gels based on Fe^{3+} and Ti^{3+} ions. During the redox process (Fullenkamp et al., 2012), the quinone-initiated radical coupling between the catechols is accompanied by the simultaneous formation of Ag^0 particles, which could be observed in the SEM image (Fig. 3). Moreover, Ag^0 particles showing in the backscattering SEM picture had diameters of approximately 500 nm and were well and uniformly dispersed within the hydrogel matrix with a narrow particle size distribution. The amount of Ag was determined by TGA analysis (Fig. S4, Supporting information). It should be noted here that a similar formation of the quinone structures between the catechol groups leading to cross-linking with IO_4^- as well as for Ag^+ was already proposed
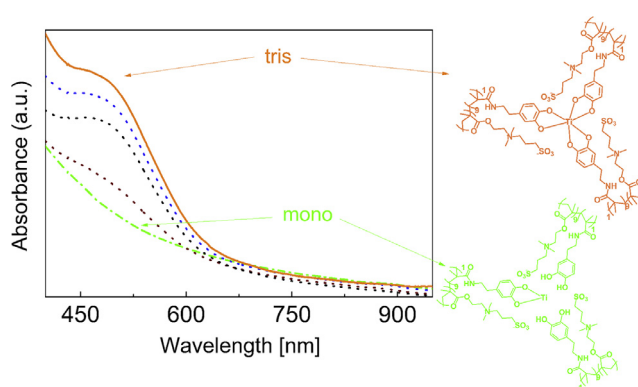

Fig. 1   UV–vis spectra of the mono-, bis-, and tris-catecholate Fe^{3+} complexes with SBE-DMA, when the pH was established at 5 (green), 8 (red) and 12 (blue).

Fig. 2   UV–vis spectra of the formation of catecholate Ti^{3+} complexes during the titration with 0.1 M NaOH (change from pH 5 to 12).
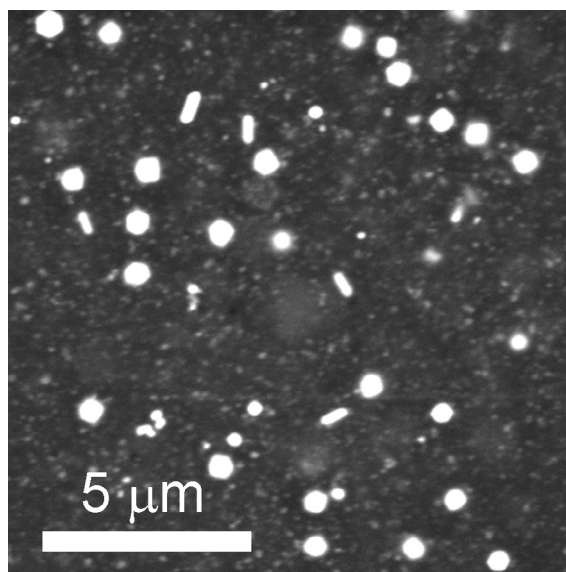
Fig. 3 SEM image of the cross section of the hydrogel based on $AgNO_3$ as a cross-linking agent.

by other authors in different systems with catecholic moieties (Brunsveld et al., 2001; Zhang et al., 2009a; Burnworth et al., 2007; Ghavami Nejad et al., 2016).

3.3. State of water determination

The hydrogel possesses several states of water, and this unique material characteristic makes such a material suitable to be utilized in biology-related fields (Vogler, 1999). Generally, in hydrogels, states of water can be divided into the freezing free, freezable-bound and non-freezing water. Freezing free water does not contribute to hydrogen bonding or complexation with polymer chains. Freezable-bond water interacts only weakly with polymer chains (Goda et al., 2006; Mirejovsky et al., 1991). Finally, non-freezing water is a fraction of the water which is bonded to the hydrophilic segments of polymer chain through hydrogen bonds and influences the biocompatibility of hydrogel (Morisaku et al., 2008).

In this study the DSC was used as the common method for the evaluation of total freezing water content (W_{tf}); that is, freezing free water combined with freezable bond water was calculated according to Eq. (2):

$$W_{tf} = \frac{\Delta H}{\Delta H_w} \cdot 100 \tag{2}$$

where ΔH is the melting enthalpy of the water in the hydrogel and ΔH_w is the melting enthalpy of water, equal to 333 J g^{-1} (Ahmad and Huglin, 1994).

The content of non-freezing water (W_{nf}) in the polymer network can be then calculated using Eq. (3) by subtraction of the total freezing water from the equilibrium water content determined by Eq. (1) after lyophilization

$$W_{nf} = \text{EWC} - W_{tf} \tag{3}$$

Fig. 4 shows the DSC curves of the first heating from −45 to 20 °C. The peaks correspond to the freezable bound and freezing free water, respectively. These data are sufficient to
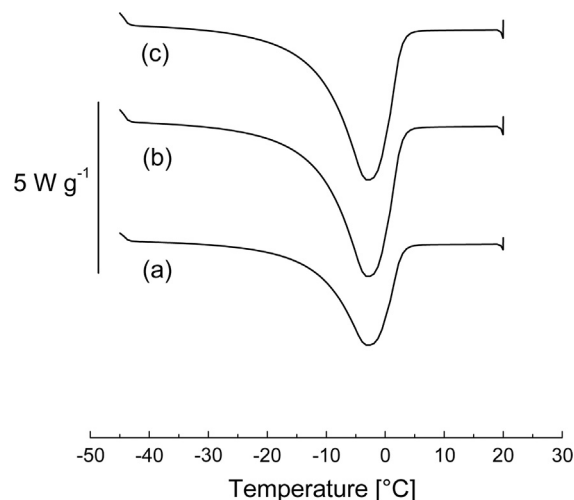

Fig. 4 DSC curves of first heating run for the Ti^{3+} SBE-DAM gel (a), Fe^{3+} SBE-DAM gel (b) and IO_4^- cross-linked SBE-DAM gel (c).

determine the melting enthalpy calculated from the area under the endothermic curves from −20 to 5 °C.

Table 1 summarizes the values of EWC, W_{tf}, and W_{nf} to compare the characteristics of the hydrogels in the presence of the various cross-linkers. Here, the Fe^{3+} cross-linked gel has the lowest value of non-freezable water content followed by the covalently cross-linked gel using IO_4^- and the Ti^{3+} cross-linked gel. Such a trend does not significantly influence the overall elasticity of the gel and the finite elasticity after recovery but considerably influences the rate of recovery (Fig. 6). It is worth noting that the water states determined for the polysulfobetaine hydrogel based on SBE showed a similar percentage of W_{nf} and higher W_{tf} (Zhang et al., 2009a). These can be attributed to the higher cross-linking density and lower hydrophilic character of the cross-linking point in our case.

3.4. Viscoelastic properties

The viscoelastic properties of the prepared Fe^{3+}-based complexes of the SBE-DAM polymer samples are shown in Fig. 5. As already mentioned, at pH 5, mono-catecholato-Fe^{3+} polymer complexes were formed. Such complexes, from the rheological point of view, behaved as a liquid because the viscous modulus (G″) prevailed over the elastic one (G′). At pH 8, when the bis-catecholato-Fe^{3+} complexes are formed

Table 1 Summarized values of state of the water determination for various hydrogels.

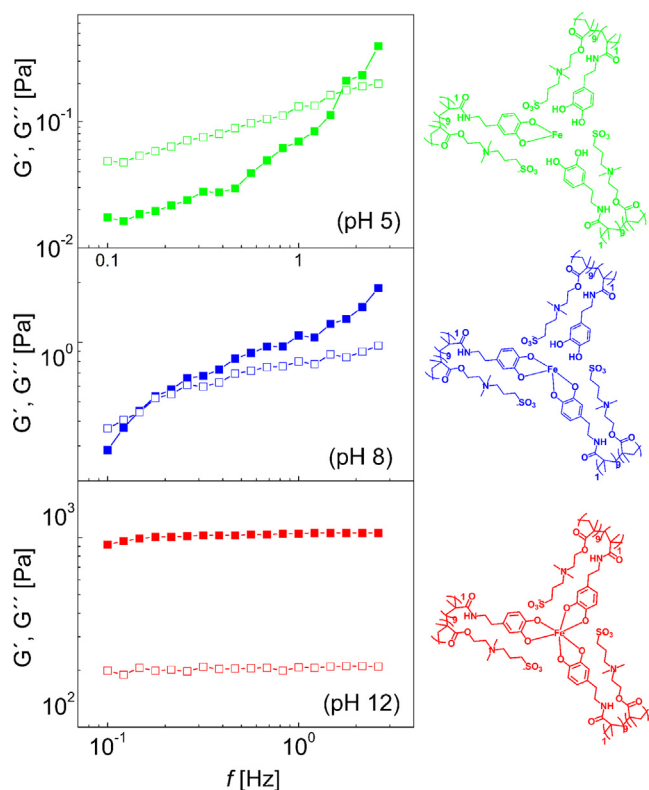| Sample	EWC (wt.%)	W_{tf} (wt.%)	W_{nf} (wt.%)
Fe^{3+} SBE-DMA gel	27.58	11.15	16.43
Ti^{3+} SBE-DMA gel	20.16	5.72	14.44
Ag^+ SBE-DMA gel	23.53	9.21	14.32
IO_4^- SBE-DMA gel	24.39	10.13	14.26

Fig. 5 Frequency dependence of the storage modulus, G' (solid symbols) and viscous modulus, G'' (open symbols) of SBE-DAM with Fe^{3+} ions exposed to various pH levels (left); proposed structure formation (right).

Fig. 6 Frequency dependence of the storage modulus, G' (solid symbols) and viscous modulus, G'' (open symbols) of SBE-DAM with Ti^{3+} ions exposed to various pH levels (left); proposed structure formation (right).

(Roberts et al., 2007), the G' started to dominate over the G'', and this effect was more pronounced at higher frequencies. Finally, at pH 12, when all the catecholic groups were complexed to tris-catecholato-Fe^{3+} complexes, a relatively stiff gel structure was formed (Lieleg et al., 2008), showing the dominance of G' over G'' in the whole frequency range. The storage modulus reached nearly 1 kPa. This value is more than four orders of magnitude higher than the value of the storage modulus for mono-catecholato-Fe^{3+}-based polymer complexes formed at pH 5 and similar to those observed by other authors for polymeric systems with catechol moieties (Holten-Andersen et al., 2011; Harrington et al., 2010; Fullenkamp et al., 2012). It should be pointed out that there is also mechanism of dopamine to form polydopamine species (Proks et al., 2013; Dreyer et al., 2012); however, in our case amine group from dopamine is transformed to amide group and it is assumed that this mechanism does not take place in present copolymer.

The viscoelastic properties of the Ti^{3+}-based complexes of the SBE-DAM samples are shown in Fig. 6. Similar to the previous case, at pH 5, a liquid-like behavior in which G'' prevailed over G' was observed. However, the addition of 0.2 eq. of 0.1 M NaOH led to a dramatic change in the rheological behavior, probably due to the much stronger attraction of Ti to the free catechol groups of the polymer and the preferable formation of tris-catecholato-Ti^{3+} complexes, providing a stiffer structure with G' dominating over G''. With the additio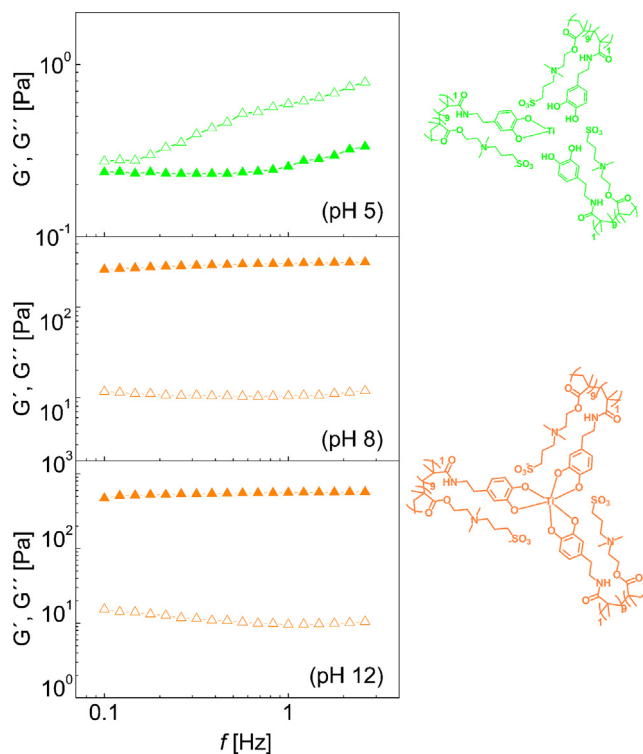nal titration with 0.1 M NaOH, the stiffness of the gel increased due to the development of the full gel structure. Thus, G' increased from 300 Pa at pH 8 to approximately 600 Pa at pH 12.

The development of the covalently Ag^+ cross-linked gel and the IO_4^- cross-linked gel is significantly time dependent. Similarly, as was described elsewhere, the Ag^+ gel formation was accomplished within the one hour. On the other hand, in the presence of IO_4^- ions, a fully crosslinked structure was obtained after 16 h, consistent with the observation for other systems (Holten-Andersen et al., 2011). Therefore, the Ti^{3+} and Fe^{3+} metal cross-linkers whose gelation takes place after a few seconds are very promising for the intended application, such as controllable adhesion.

For comparison, the rheological investigation of both IO_4^- and Ag^+ covalently cross-linked gels was investigated and is shown in Fig. 7. At pH 5, before the addition of the cross-linking agent, the polymer exhibited nearly Newtonian behavior. After the addition of IO_4^- as the cross-linking agent, the full gelation process was completed after 5 h, while, in the case of Ag^+, the gelation process for the sample with the lowest amount of cross-linker was complete after 45 min. The rate of gelation increased with amount of Ag^+ ions. Generally, by comparison of the chemically crosslinked systems and the systems cross-linked by the formation of complexes with metal ions, it can be concluded that the Ti^{3+} and Fe^{3+} metal cross-linked gels show similar rheological performance parameters to the covalently cross-linked gels; however, the complete gelation process is significantly faster in the case of non-covalent crosslinking.
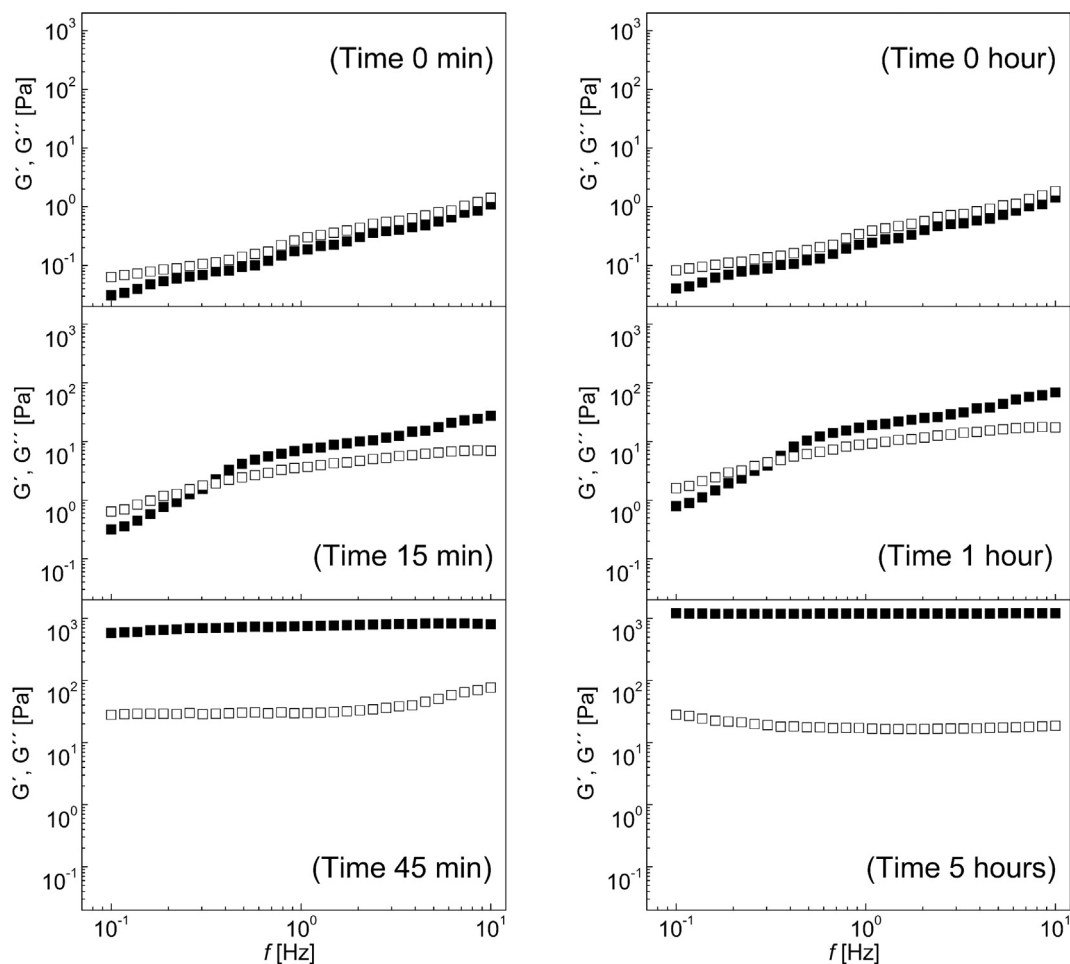
Fig. 7   Frequency dependence of the storage modulus, G' (solid symbols) and viscous modulus, G'' (open symbols) of the Ag^+ cross-linked SBE-DMA gel (left) and IO_4^- cross-linked SBE-DMA gel (right) at various cross-linking periods.

Another advantage of the non-covalently cross-linked gels can be the reversibility of the gelation process. The reversibility was observed after the introduction of the EDTA solution as a chelating agent to the Fe^{3+} cross-linked gel. As Fig. 8 clearly shows, the viscoelastic moduli significantly changed their dependence on the applied frequency, and the viscous modulus overcame the elastic one, confirming the disruption of the created gel-like structure.

3.5. Self-healing behavior

The self-healing behavior of the Fe^{3+} metal cross-linked gels in a macroscopic view is shown in Scheme 2. The hydrogel from tris-catecholato-Fe^{3+} complex after preparation is presented in Scheme 2a. After cutting the sample, the hydrogel was definitively divided into two individual parts (Scheme 2b). However, when the individual parts were held together, the material reverted to the uniform hydrogel (Scheme 2c). Due to the self-healing ability, and especially for the metal cross-linked gels, the structure was fully recovered in several seconds as was further confirmed by viscoelastic investigations (Fig. 9).

To compare the deformation and self-healing capabilities of the gels, the G' was normalized to the values at linear
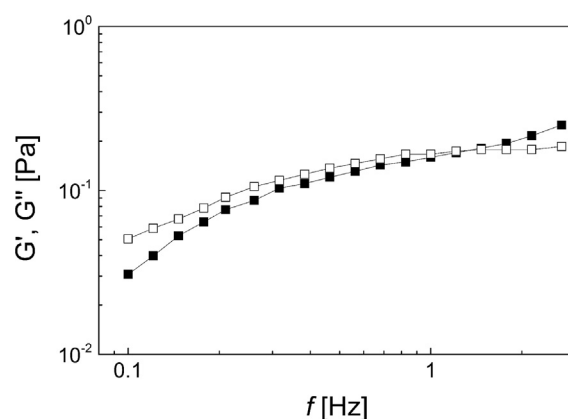

Fig. 8   Frequency dependence of the storage modulus, G' (solid symbols) and viscous modulus, G'' (open symbols) of the Fe^{3+} cross-linked SBE-DMA gel at pH 12 after the addition of the EDTA solution.

conditions measured before deformation (Ahmad and Huglin, 1994).

As Fig. 9 (left) shows, all samples exhibited stable behavior at small deformations. The sample consisting of the polymer

Scheme 2   The Fe^{3+} metal cross-linked gels at pH 12 (a) the cut gel (b) and recovered (c).
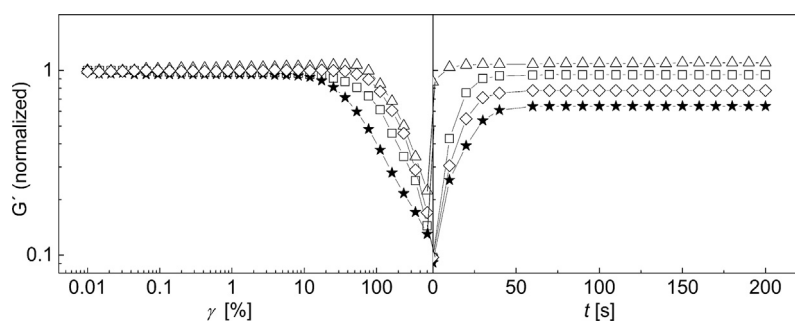

Fig. 9   Recovery test for the Ti^{3+} SBE-DAM gel (Δ), Fe^{3+} SBE-DAM gel (□), Ag^+ SBE-DAM gel (◇) and $NaIO_4$ SBE-DAM gel (★).

covalently cross-linked in the presence of IO_4^- had the lowest stability, followed by the Fe^{3+} cross-linked gel and the Ag^+ chemically cross-linked gel, and the resistance against deformation was highest for the Ti^{3+} cross-linked gel. The deformation finished at 500%, where the structures of almost all the gels were destroyed. Immediately after reaching this value, the measurement was set up for linear conditions and the recovery behavior of the gels was investigated (Fig. 9 (right)). The worst self-healing properties were observed for the hydrogel based on covalent bonding with IO_4^- (only 65%), followed by the sample with the Ag^+ cross-linker (73%) due to the presence of the covalent quinonic cross-linking in the hydrogel. The Fe^{3+} cross-linked hydrogel showed relatively good recovery, and, after 200 s, the sample reached 94% of the total elastic modulus. The Ti^{3+} cross-linked gel had a very fast response and a nearly immediate self-healing process took place when the 100% of the total elastic modulus was reached. Thus, it can be concluded that, thanks to the coordinative crosslinking behavior, the metal ligand-based gels have excellent recoverability in comparison with the covalently crosslinked gels.

3.6. Antibacterial assessment

Regardless of the slower gelation process and inferior self-healing properties in comparison with the Fe^{3+} and Ti^{3+} cross-linked gels, the advantage of the covalently cross-linked gel based on Ag^+ is the formation of the Ag^0 particles during the gelation process and their homogeneous dispersion within the gel. Such a material can provide excellent antibacterial activity both in solution and on a surface. Therefore, the antibacterial properties of the gel in solution were assessed by exposure of a suspension of the gram-negative bacteria *E. coli* and gram-positive *S. Aureus* to the Ag^+ hydrogel, and an aliquot was seeded for cultivation for approximately 16 h. Different amounts of Ag contents demonstrated the

capability of adjusting the antibacterial performance (Table 2). The hydrogel with highest Ag contents showed only 0.6% live cells of *E. coli* compared to the negative control sample on a hydrogel without Ag content and 8.1% live cells of *S. Aureus*. In the case of hydrogels with 7.5 and 5% Ag content, the ability of the *E. coli* cells to achieve colony formation increases to 1.8 and 7.2%, respectively. In case of *S. Aureus* cells to achieve such colony formation increase to 14.9 and 19.4%, respectively. It can be noted that similar antibacterial properties were observed in the reaction of the sulfobetaine based hydrogel with catecholic modification with Ag^+ ions (Ham et al., 2011).

The antibacterial activity of 5 mg of hydrogels on the *E. coli* and *S. Aureus* seeded medium surface was studied by the determination of the zones of inhibition against *E. coli* and *S. Aureus*, which are visualized in Fig. 10. The sample with the highest contents of Ag in the hydrogel displayed an inhibition zone area of $33 \pm 3 \text{ mm}^2$ and $32 \pm 2.5 \text{ mm}^2$ for *E. coli* and for *S. Aureus*, respectively. Decreasing the Ag^0 content to 7.5 and 5% in the hydrogel led to inhibition zone areas of 21 ± 1.6 and $14 \pm 1.2 \text{ mm}^2$, respectively, for *E. coli* and 19.6 ± 0.9 and $11.9 \pm 0.7 \text{ mm}^2$, respectively for *S. Aureus*.

3.7. Cytotoxicity evaluation

In the view of the possible utilization of this system for *in vivo* applications, material cytotoxicity test was performed. Thus, neat SBE-DAM was treated with culture medium and the extract was applied to the NIH/3T3 mouse embryonic fibroblast cell line in a concentration range from 10 mg mL^{-1} to 200 mg mL^{-1}. After 48 h of incubation, the cellular viability was determined by the MTT assay, and the results are plotted in Fig. 11 left. In the whole concentration range, the cell viability was considerably above 80%, which is assigned as showing no cytotoxicity. Moreover, no change in the morphology of the cells was observed. In case of direct method using human

Table 2 Composition and antibacterial properties of Ag^+ cross-linked hydrogels.

Ag^0 content in hydrogel (wt.%)[a]	*S. Aureus* Colony forming units (cfu) per OD 0.00028	% Of alive cells	*E. Coli* Colony forming units (cfu) per OD 0.00028	% Of alive cells
0	314,167 ± 4444	100	356,667 ± 5556	100
5	61,100 ± 2267	19.4	25,633 ± 1001	7.2
7.5	46,967 ± 2356	14.9	6450 ± 328	1.8
10	25,600 ± 933	8.1	2017 ± 176	0.6

[a] Based on TGA analysis (Fig. S4, Supporting information).
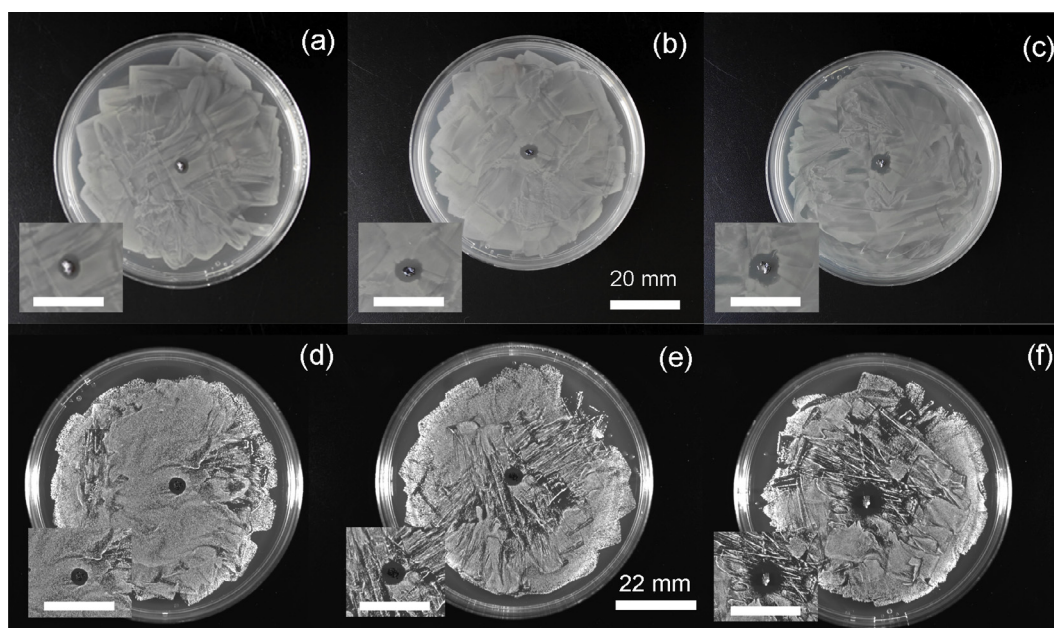

Fig. 10 Inhibition zones for samples with (a) 5%, (b) 7.5% and (c) 10% of Ag used for cross-linking for *E. Coli* and (d) 5%, (e) 7.5% and (f) 10% of Ag used for cross-linking for *S. Aureus*. Scale bar in the figure insets represents 13 mm.
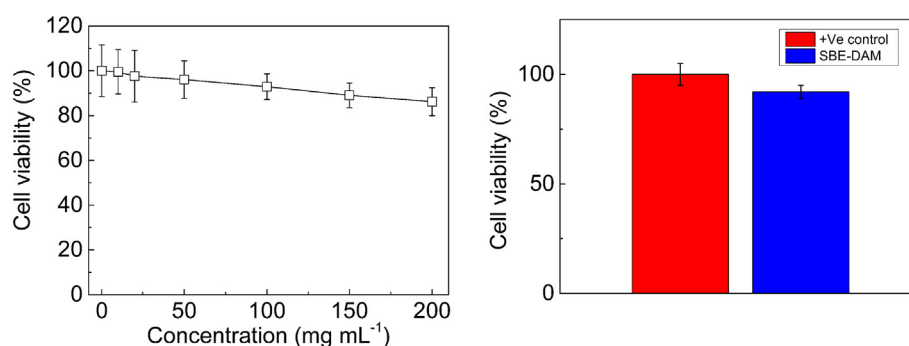

Fig. 11 Cell viability for extract method of the SBE-DMA on the NIH/3T3 mouse embryonic fibroblast cell line (left) and cell viability for direct method of human dermal fibroblast cell (F121) (right).

dermal fibroblast cell (F121) the cell viability was found to be 92% with respect to the positive control. Again no significant changes were observed on the cells. Therefore, it can be stated that the SBE-DMA copolymer provides a promising material capable controlled release, self-healing and good loading capacity.

4. Conclusion

The sulfobetaine-based copolymer (SBE-DAM) was synthesized by a free radical reaction of [2-(methacryloyloxy)ethyl]dimethyl-(3-sulfopropyl)ammonium betaine (SBE) and

dopamine methacrylamide (DAM) and was used as a platform for hydrogel formation by the presence of various metal ions (Ti^{3+}, Fe^{3+}, Ag^+) and pH levels. The coordination of catechol units in the copolymer with Ti^{3+} and Fe^{3+} ions led to the formation of hydrogels tunable by pH. UV–vis measurements confirmed the formation of the hydrogels with more coordination stable catecholate moieties at higher pH values. Viscoelastic measurements showed that non-covalently cross-linked Ti^{3+}, Fe^{3+}-based hydrogels exhibited similar values of elastic modulus as the covalently cross-linked Ag^+ or IO_4^--based ones. The reversibility of Ti^{3+}, Fe^{3+}-based coordination crosslinking was proven by the addition of EDTA as a strong coordination agent. The investigation on the self-healing ability of the SBE-DMA based hydrogel showed full recovery in the case of Ti^{3+} and 92% recovery in the case of Fe^{3+}-based hydrogels. In contrast, the covalently based gels exhibited maximally 72% recovery. On the contrary to Ti^{3+} and Fe^{3+}, the Ag^+ led to covalent crosslinking with entrapped Ag ions, as confirmed by SEM images. The antimicrobial performance of the hydrogel can be tuned by the amount of the Ag^0 formed in the hydrogel. Finally, it was proven that SBE-DAM was classified as non-toxic when cell viability was kept considerably above 80% at all investigated concentrations and 92% for direct contact method with SBE-DAM copolymer. The hydrogel based on SBE-DAM enabling the adjustment of antibacterial properties while at the same time possessing non-toxic behavior shows potential to be used for water treatment and medical applications.

Acknowledgments

Appendix A. Supplementary material

Supplementary data associated with this article can be found, in the online version, at http://dx.doi.org/10.1016/j.arabjc.2017.03.009.

References

Ahmad, M.B., Huglin, M.B., 1994. DSC Studies on states of water in cross-linked poly(methyl methacrylate-co-n-vinyl-2-pyrrolidone) hydrogels. Polym. Int. 33, 273–277.

Bassett, D.C., Hati, A.G., Melo, T.B., Stokke, B.T., Sikorski, P., 2016. Competitive ligand exchange of crosslinking ions for ionotropic hydrogel formation. J. Mater. Chem. B 4, 6175–6182.

Brunsveld, L., Folmer, B.J.B., Meijer, E.W., Sijbesma, R.P., 2001. Supramolecular polymers. Chem. Rev. 101, 4071–4097.

Burnworth, M., Knapton, D., Rowan, S.J., Weder, C., 2007. Metallo-supramolecular polymerization: a route to easy-to-process organic/inorganic hybrid materials. J. Inorg. Organomet. Polym Mater. 17, 91–103.

de Greef, T.F.A., Meijer, E.W., 2008. Materials science – supramolecular polymers. Nature 453, 171–173.

Dreyer, D.R., Miller, D.J., Freeman, B.D., Paul, D.R., Bielawski, C. W., 2012. Elucidating the structure of poly(dopamine). Langmuir 28, 6428–6435.

Fletcher, N.L., Lockett, C.V., Dexter, A.F., 2011. A pH-responsive coiled-coil peptide hydrogel. Soft Matter 7, 10210–10218.

Freitas, L.L.D., Stadler, R., 1987. Thermoplastic elastomers by hydrogen-bonding. 3. Interrelations between molecular-parameters and rheological properties. Macromolecules 20, 2478–2485.

Fullenkamp, D.E., Rivera, J.G., Gong, Y.K., Lau, A.K.H., He, L., Varshney, R., Messersmith, P.B., 2012. Mussel-inspired silver-releasing antibacterial hydrogels. Biomaterials 33, 3783–3791.

Ghavami Nejad, A., Park, C.H., Kim, C.S., 2016. In situ synthesis of antimicrobial silver nanoparticles within antifouling zwitterionic hydrogels by catecholic redox chemistry for wound healing application. Biomacromolecules 17, 1213–1223.

Gil, E.S., Hudson, S.M., 2004. Stimuli-responsive polymers and their bioconjugates. Prog. Polym. Sci. 29, 1173–1222.

Goda, T., Watanabe, J., Takai, M., Ishihara, K., 2006. Water structure and improved mechanical properties of phospholipid polymer hydrogel with phosphorylchlorine centered intermolecular crosslinker. Polymer 47, 1390–1396.

Guvendiren, M., Lu, H.D., Burdick, J.A., 2012. Shear-thinning hydrogels for biomedical applications. Soft Matter 8, 260–272.

Ham, H.O., Liu, Z.Q., Lau, K.H.A., Lee, H., Messersmith, P.B., 2011. Facile DNA immobilization on surfaces through a catecholamine polymer. Angew. Chem. Int. Ed. 50, 732–736.

Harrington, M.J., Masic, A., Holten-Andersen, N., Waite, J.H., Fratzl, P., 2010. Iron-clad fibers: a metal-based biological strategy for hard flexible coatings. Science 328, 216–220.

Hoeben, F.J.M., Jonkheijm, P., Meijer, E.W., Schenning, A., 2005. About supramolecular assemblies of pi-conjugated systems. Chem. Rev. 105, 1491–1546.

Holten-Andersen, N., Fantner, G.E., Hohlbauch, S., Waite, J.H., Zok, F.W., 2007. Protective coatings on extensible biofibers. Nat. Mater. 6, 669–672.

Holten-Andersen, N., Mates, T.E., Toprak, M.S., Stucky, G.D., Zok, F.W., Waite, J.H., 2009. Metals and the integrity of a biological coating: the cuticle of mussel byssus. Langmuir 25, 3323–3326.

Holten-Andersen, N., Harrington, M.J., Birkedal, H., Lee, B.P., Messersmith, P.B., Lee, K.Y.C., Waite, J.H., 2011. PH-induced metal-ligand cross-links inspired by mussel yield self-healing polymer networks with near-covalent elastic moduli. Proc. Natl. Acad. Sci. USA 108, 2651–2655.

Ilcikova, M., Tkac, J., Kasak, P., 2015. Switchable materials containing polyzwitterion moieties. Polymers 7, 2344–2370.

Jin, Q., Chen, Y., Wang, Y., Ji, J., 2014. Zwitterionic drug nanocarriers: a biomimetic strategy for drug delivery. Colloid Surf. B 124, 80–86.

Kasák, P., Kroneková, Z., Krupa, I., Lacík, I., 2011. Zwitterionic hydrogels crosslinked with novel zwitterionic crosslinkers: synthesis and characterization. Polymer 52, 3011–3020.

Lee, B.P., 2008. Biomimetic compounds and synthetic method therefor. PCT Int. Appl., WO 2008019352.

Lee, H., Scherer, N.F., Messersmith, P.B., 2006. Single-molecule mechanics of mussel adhesion. Proc. Natl. Acad. Sci. USA 103, 12999–13003.

Li, A., Mu, Y., Jiang, W., Wan, X., 2015. A mussel-inspired adhesive with stronger bonding strength under underwater conditions than under dry conditions. Chem. Commun. 51, 9117–9120.

Lia, G., Cheng, G., Xue, H., Chen, S., Zhang, F., Jiang, S., 2008. Ultra low fouling zwitterionic polymers with a biomimetic adhesive group. Biomaterials 29, 4592–4597.

Lieleg, O., Claessens, M., Luan, Y., Bausch, A.R., 2008. Transient binding and dissipation in cross-linked actin networks. Phys. Rev. Lett. 101, 108101.

Mart, R.J., Osborne, R.D., Stevens, M.M., Ulijn, R.V., 2006. Peptide-based stimuli responsive biomaterials. Soft Matter 2, 822–835.

Mirejovsky, D., Patel, A.S., Rodriguez, D.D., 1991. Effect of proteins on water and transport-properties of various hydrogel contact-lens materials. Curr. Eye Res. 10, 187–196.

Morisaku, T., Watanabe, J., Konno, T., Takai, M., Ishihara, K., 2008. Hydration of Phosphorylcholine groups attached to highly swollen polymer hydrogels studied by thermal analysis. Polymer 49, 4652–4657.

Mrlík, M., Ilčíková, M., Cvek, M., Pavlínek, V., Zahoranová, A., Kroneková, Z., Kasak, P., 2016. Carbonyl iron coated with sulfobetaine moiety as a biocompatible system and the magnetorheological performance of its silicone oil suspensions. RSC, Adv. 6, 32823–32830.

Pei, Y., Trava-Sejdic, J., Williams, D.E., 2012. Reversible electrochemical switching of polymer brushes grafted onto conducting polymer films. Langmuir 28, 8072–8083.

Phadke, A., Zhang, C., Arman, B., Hsu, C.C., Mashelkar, R.A., Lele, A.K., Tauber, M.J., Arya, G., Varghese, S., 2012. Rapid self-healing hydrogels. Proc. Natl. Acad. Sci. USA 109, 4383–4388.

Piest, M., Zhang, X.L., Trinidad, J., Engbersen, J.F.J., 2011. PH-responsive, dynamically restructuring hydrogels fyrmed by reversible crosslinking of PVA with phenylboronic acid functionalised PPO-PeO-PPO spacers (Jeffamines (R)). Soft Matter 7, 11111–11118.

Pop-Georgiewski, O., Popelka, S., Houska, M., Chvostova, D., Proks, V., Rypacek, F., 2011. Poly(ethylene oxide) layers grafted to dopamine-melanin anchoring layer: stability and resistance to protein adsorption. Biomacromol 12 (9), 3232–3242.

Proks, V., Brus, J., Pop-Georgiewski, O., Vecernikova, E., Wisniewski, W., Kotek, J., Urbanova, M., Rypacek, F., 2013. Thermal-induced transformation of polydopamine structures: an efficient route for the stabilization of the polydopamine surfaces. Macromol. Chem. Phys. 214, 499–507.

Roberts, M.C., Hanson, M.C., Massey, A.P., Karren, E.A., Kiser, P.F., 2007. Dynamically restructuring hydrogel networks formed with reversible covalent crosslinks. Adv. Mater. 19, 2503–2507.

Roy, D., Cambre, J.N., Sumerlin, B.S., 2010. Future perspectives and recent advances in stimuli-responsive materials. Prog. Polym. Sci. 35, 278–301.

Sedó, J., Saiz-Poseu, J., Busqué, F., Ruiz-Molina, D., 2013. Catechol-based biomimetic functional materials. Adv. Mater. 25, 653–701.

Sin, M.-C., Sun, Y.-M., Chang, Y., 2014. Zwitterionic-based stainless steel with well-defined polysulfobetaine brushes for general bioadhesive control. ACS Appl. Mat. Inter. 6, 861–873.

Sobolčiak, P., Kasák, P., Lacík, I., 2011. Polysulfobetaines: synthesis, properties in water systems and applications. Chem. Papers 105, 918–925.

South, A.B., Lyon, L.A., 2010. Autonomic self-healing of hydrogel thin films. Angew. Chem. – Int. Ed. 49, 767–771.

Stach, M., Kroneková, Z., Kasák, P., Kollár, J., Pentrák, M., Mičušík, M., Chorvát Jr., D., Nunneyd, T.S., Lacík, I., 2011. Polysulfobetaine films prepared by electrografting techniqe for reduction of biofouling on electroconductive surfaces. Appl. Surf. Sci. 257, 10795–10801.

Stadler, R., Freitas, L.D., 1986. Thermoplastic elastomers by hydrogen bonding. 1. Rheological properties of modified polybutadiene. Colloid Polym. Sci. 264, 773–778.

Sundaram, H.S., Han, X., Nowinski, A.K., Ella-Menye, J.R., Wimbish, C., Marek, P., Senecal, K., Jiang, S.Y., 2014. One-step dip coating of zwitterionic sulfobetaine polymers on hydrophobic and hydrophilic surfaces. ACS Appl. Mat. Inter. 6, 6664–6671.

Vogler, E.A., 1999. Water and the acute biological response to surfaces. J. Biomater. Sci. – Polym. Ed. 10, 1015–1045.

Xu, Z., 2013. Mechanics of metal-catecholate complexes: the roles of coordination state and metal types. Sci. Rep. 3, 2914.

Yan, M., Ge, J., Dong, W., Liu, Z., Ouyang, P., 2006. Preparation and characterization of a temperature-sensitive sulfobetaine polymer-trypsin conjugate. Biochem. Eng. J. 30, 48–54.

Yang, W., Sundaram, H.S., Ella, J.R., He, N., Jiang, S., 2016. Low-fouling electrospun PLLA films modified with zwitterionic poly (sulfobetaine methacrylate)-catechol conjugates. Acta Biomater. 40, 92–99.

Yavvari, P.S., Srivastava, A., 2015. Robust, self-healing hydrogels synthesised from catechol rich polymers. J. Mater. Chem. B 3, 899–910.

Yu, L., Liu, X., Yuan, W., Brown, L.J., Wang, D., 2015. Confined flocculation of ionic pollutants by poly(l-dopa)-based polyelectrolyte complexes in hydrogel beads for three-dimensional. Quant., Efficient Water Decontamination, Langmuir 31, 6351–6366.

Zeng, H.B., Hwang, D.S., Israelachvili, J.N., Waite, J.H., 2010. Strong reversible Fe^{3+}-mediated bridging between dopa-containing protein films in water. Proc. Natl. Acad. Sci. USA 107, 12850–12853.

Zhang, Z., Chen, S., Chang, Y., Jiang, S., 2006. Surface grafted sulfobetaine polymers via atom transfer radical polymerization as superlow fouling coatings. J. Phys. Chem. B 110, 10799–10804.

Zhang, Z., Finlay, J.A., Wang, L., Gao, Y., Callow, J.A., Callow, M.E., Jiang, S., 2009a. Polysulfobetaine-grafted surfaces as environmentally benign ultralow fouling marine coatings. Langmuir 25, 13516–13521.

Zhang, Z., Chao, T., Liu, L.Y., Cheng, G., Ratner, B.D., Jiang, S., 2009b. Zwitterionic hydrogels: an in vivo implantation study. J. Biomater. Sci. – Polym. Ed. 20, 1845–1859.